# The $\nu_6, \nu_7, \nu_8$ and $\nu_{10}$ Bands of $HO_2NO_2$

Randall R. Friedl and Randy D. May
Jet Propulsion Laboratory
California Institute of Technology
4800 Oak Grove Drive
Pasadena, CA 91109

and

Geoffrey Duxbury
Department of Physics and Applied Physics
University of Strathclyde
John Anderson Building
107 Rottenrow
Glasgow G4 ONG, Scotland U.K.

Number of manuscript pages: 30

Number of Figures: 6

Number of Tables: 4

Running Title: The $\nu_6, \nu_7, \nu_8$ and $\nu_{10}$ Bands of $HO_2NO_2$

Mail correspondence to: Dr. Randall R. Friedl
Jet Propulsion Laboratory
California Institute of Technology
4800 Oak Grove Drive
Pasadena, CA 91109

List of Symbols

$\nu$ - Greek l.c. nu

$\mu$ - Greek l.c. mu

$\kappa$ - Greek l.c. kappa

A - Greek u.c. delta

$\xi$ - Greek l.c. xi

**Abstract**

Two ncw fundamental vibration rotation bands have been observed for H02N02 and assigned. They arc $\nu_7$ at 648 cm-l and $\nu_8$ at 466.7 cm-l. On the basis of these assignments the previously observed bands at 722 $cm^{-1}$, 801.5 $cm^{-1}$ and at 919 $cm^{-1}$ arc assigned toV10, $V_7$ + v 12 and to 2 $\nu_8$, respectively. A partial rotational analysis of the atmospherically relevant $\nu_6$ band has been carried out and the effects of tunnelling, Coriolis interactions, and hot bands on the rotational structure have been characterized. The band origin derived from this analysis is 802.543 $cm^{-1}$.

**introduction**

Model calculations of atmospheric ozone depletion duc to chlorofluorocarbon degradation or possible commercial operation of stratospheric aircraft are particularly sensitive to processes that effect the partitioning between reactive $NO_x$ (NO, N02, and N03) and reservoir $NO_Y$ ($HNO_3$, N205, $HO_2NO_2$, C1ONO2, and $CH_3CO_3NO_2$) species. As a dramatic example of this sensitivity, the recent inclusion into models of the the reaction N205 + H20, assumed to occur on the global sulfate layer, has resulted in a great reduction of the predicted ozone depletion duc to a proposed fleet of stratospheric aircraft (1). Recent attempts to further understand atmospheric $NO_y$ partitioning have focused on laboratory investigations of nitrogen oxide chemistry as well as atmospheric observations of the relevent species.

Peroxynitric acid, (PNA), H02N02 is an important, albeit poorly studied, temporary reservoir species of '$NO_x$ and $HO_x$ in the stratosphere (2). It is formed by the reaction of H02 with N02

$$H02 + N02 + M \rightarrow H02N02 + M \qquad (1)$$

and removed primarily by photolysis and reaction with OH. The PNA removal processes are thought to reform H02 and N02, however, the product 'distributions have not yet been fully characterized. The existence of PNA reaction channels leading to HN03 could dramatically affect the partitioning between $NO_Y$ species since the midlatitude lifetime of HN03 ($\approx$ 30 days at 20 km) is much longer than H02N02 ($\approx$ 2 days).

Atmospheric observations of PNA and HN03 can provide important constraints on atmospheric models of $NO_Y$ chemistry. Recently, fourier transform infrared spectra of the stratosphere obtained using balloon borne (3) and space shuttle borne (4) spectrometers have exhibited spectral features near 803 $cm^{-1}$ that are attributed to PNA. The retrieval of precise atmospheric PNA abundances from this data has been hampered, however, by the lack of line. parameters for the 803 $cm^{-1}$ band, and the absence of any direct measurements of the low frequency infrared bands responsible for some of the overtone and hot band structure in this region. Recently, in an attempt to facilitate the retrieval of PNA abundances from atmospheric

spectra, wc have obtained PNA absorption coefficients for the 803 cm-l band at 220 K (5) Although this data is useful for calculating PNA absorption coefficients over a range of pressures and at a temperature more relevant to the atmospheric observations it dots not provide for a completely satisfactory analysis of the atmospheric spectra.

In the present work wc have attempted to further characterize the complex vibration-rotation structure of the $\nu_6$ band of PNA at 803 $cm^{-1}$. To that end wc have identified several low frequency fundamental vibration-rotation bands of PNA. The frequencies of the band origins have been used to obtain ncw insights into the assignment of the high resolution spectrum of the $\nu_6$ band obtained by us earlier (5).

**Experimental and Computational Techniques**

The methods used to prepare and observe PNA have been discussed previously (5,6) Briefly, H02N02 was prepared in the liquid phase using the method of Kenley et al (7).

$$H202\ (90\%) + NO_2BF_4\ (s) \rightarrow H02N02 + HBF_4 \qquad (2)$$

Samples were prepared in 5 ml. quantities and transferred to the inlet of either a multipass (White type) absorption cell attached to a Bomem DA3-002 FTS or to a Herriott cell attached to a tunable diode laser spectrometer. Spectra were recorded over a range of temperatures from room temperature to 220 K, At the lower temperatures PNA condensed on to the wall of the absorption cells, and the gas phase PNA concentration remained approximately at the 220 K equilibrium vapor pressure (3.5 mtorr).

Infrared spectra taken on the FTS system were obtained as described by May and Friedl (5) with the following exceptions: the KCl beamsplitter was replaced by a 3 $\mu$m Mylar beamsplitter; the White cell and spectrometer window materials were changed from KC] to KRS-5. In order to optimize the recording of the FTIR spectra simultaneous measurements of the ultraviolet spectra of the H02N02 sample were made using a diode array spectrometer. It

was found that in the low temperature experiments spectra of PNA with very small impurity concentrations could be recorded. Total cell pressures ranged from 0.0S to 0.1 torr.

The diode laser measurements used the spectrometer described by May and Webster (6) which was coupled to a 30 pass 1 m Herriott cell. This was used to record selected regions of the 803 cm-' band at Doppler limited resolution.

The initial simulations of the $\nu_6$ band structure were made using a version of the Birss and Ramsay band contour program (8), as modified by Judge (9) and Duxbury (10). Later calculations in which the effects of tunneling and Coriolis coupling were included were carried out using the program described by Pickett (Ii).

**Results**

*Observation of New Fundamental Bands of $HO_2NO_2$*

Prior to the present study, only the center frequencies of the $\nu_1, \nu_2, \nu_3, \nu_4, \nu_5, \nu_6$ and $\nu_1$ 2 bands had been determined experimentally (12-14) As a result, thermodynamic calculations of the heat capacity and entropy had relied largely on vibration frequencies derived from ab-initio calculations (15). However, a comparison of these calculated frequencies with observed frequencies of the isoelectronic molecule $FNO_3$ (16) led to the suggestion that some of the calculated fundamental vibrational frequencies might be rather inaccurate. We have therefore carried out measurements of the vibrational spectrum from 350 to 900 $cm^{-1}$ at room temperature and at 220 K to try to locate more of the low lying vibrational fundamentals.

As a result of these new measurements, coupled with a reassignment of part of the high resolution spectrum which wc obtained previously, wc believe that wc have now identified and measured the vibrational origins of three additional fundamental vibrations. The 722 $cm^{-1}$ band observed by May and Petersen (13) is now assigned as $\nu_{10}$, (of A" symmetry in the near symmetry group for this molecule, $C_s$.) This is close to that of the equivalent N02 wagging motion in FON02 of 708.5 $cm^{-1}$ (16). Two ncw weak bands at 648 and 466.7 $cm^{-1}$ have been observed. Based upon a comparison with other bands known to belong to H02N02, the bands

at 648 $cm^{-1}$ (see Figure 1) and 466.7 $cm^{-1}$ arc assigned to $\nu_7$, (NO stretch), and $\nu_8$ (N02 rock). Using the values of the vibration frequencies of these newly determined fundamentals, the combination or overtone bands at 801.5 $cm^{-1}$ and 919 cm-' arc assigned to v7 + $\nu_{12}$ and 2 $\nu_8$, respectively. (SCC Table I)

On the basis of our spectra, and bearing in mind the frcqucncics of the equivalent bands of $FONO_2$, wc believe that the remaining bands v9, the NOO deformation, and $\nu_{11}$, the OH torsion, must both lic below 350 $cm^{-1}$ which is the current limit of our observations. Since the low frequency vibrational states have an appreciable thermal population at stratospheric temperatures of about 220 K, the final modelling of the $\nu_6$ band requires that the two remaining fundamental bands bc identified,

*The $\nu_6$ band*

The v6 band at 802,54 cm-l has a complex rotational structure. The band is associated with the N02 scissors vibration and lies c1osc in wavenumber to that of the equivalent onc observed in FON02 at 803.7 $cm^{-1}$. The spectrum of the v6 band of PNA has been recorded using Fourier transform spectrometers at the Rutherford Appleton Laboratory by Bell and Ballard (17,1 8) and at JPL by May and Friedl (5) and by May and Peterson (13) both at room temperature and at 220 K. High resolution diode laser spectra of portions of the band have also been recorded by May (19).

The microwave spectrum of PNA was analyzed by Suenram, Lovas and Pickett (20). They showed that the molecule was a rather asymmetric near prolate top and was non-planar, with tunnelling motion associated with the hydrogen atom. The heavy atom framework is planar, and the near symmetry group is therefore $C_s$. The Hamiltonian used for that work is described in detail by Pickett (21), and includes the effects of tunnelling between the inversion states of the non-planar structure.

Rotational transitions in the Q branch of the $\nu_6$ band arc largely unresolved even at the doppler limit. In order to account for the degradation of the band to higher cm-l, wc find that

the A rotational constant in the excited state needs to be greater than that of the ground state by ca. 0.001 $cm^{-1}$.[18] The partially "resolved rotational structure calculated for the Q branch is sensitive to the values of B and of C". In addition, the initial modeling efforts on the Q branch suggested that the effects of tunnelling splitting would be small (18).

The P and R branches of the $\nu_6$ band exhibit some regular structure CIOSC to the band origin. Although the lowest J transitions arc too weak to be easily identified, analysis of a synthetic A-type spectrum of the low J parts of the P and R branches showed that two types of regular structure arc predicted, C-type and A-type. $HO_2NO_2$ is quite an asymmetric near prolate rotor with a value of the Ray asymmetry parameter, $\kappa \approx -0.7$. This large departure from the symmetric rotor limiting value of -1,0 results in a rapid switchover from prolate to oblate rotor pattern of the energy levels associated with the lowest $K_a$ values for a given J, i.e. $J_{0J}$ and $J_{1J}$ ($J_K$ K ) become degenerate when J -10 or greater. As a result, lines with a characteristic spacing of 2C arc observed in the spectrum. This is shown in Figure 3. Analysis of this series of lines enabled the band origin to be determined. (see Table II)

The second series of regularly-spaced lines is associated with transitions between levels having J - $K_a$. These lines show little asymmetry splitting and hence correspond to a typical "symmetric rotor" pattern with a characteristic spacing of ( B -t- C ). The "beating" between this series and the "2C" series confirms the location of the band origin, In addition, the identification of the two series of lines resulted in an initial estimate of the A, B , and C rotational constants for the $\nu_6$ state.

In addition to the regular patterns of lines observed in the low J region of the P and R branches, a large number of weaker lines arc observed in the low J region and a rather irregular pattern of lines in the high J region. Test calculations carried out for the low J region showed that most of the weaker lines can be accounted for if the $\nu_6$ band is an A:B hybrid with a substantial B component. However, using the standard non-rigid asymmetric rotor analysis wc were unable to rcproducc the rapid switchover to a complex rotational pattern at J values of ca. 20. As stated above, Suenram, Lovas and Pickett have shown that in the ground state

peroxynitric acid is non-planar, with tunnelling between the two conformers. Application of this model to the excited state led us to the possibility that even at the lower resolution of the infrared spectra, some of the complications manifest in the P and R branches of the spectra might be due to changes in the tunneling with vibrational state.

In order to explore the influence of the tunnelling states, three hypotheses were investigated, namely, that the centrifugal distortion constants vary significantly with vibrational state, that the size of the effective Coriolis coupling constant between the ground and the excited tunneling states varies as a function of vibrational state, and that the separation of the tunnelling states varies with vibrational level. The low J transitions should exhibit a significant tunnelling splitting if there is a marked vibrationally induced change in the separation of the tunnelling states, This possibility can be discounted since the experimental spectra shown in Figure 4 show no evidence for such a splitting. Inclusion of vibrationally dependent distortion constants or coupling between the tunnelling states dots produce a considerable spreading of the K structure for high J levels, although not as rapidly as is observed experimentally (SCC Figure 5). This spreading can be made to occur in the calculated spectra either by varying the largest centrifugal distortion constant, AK, or the effective Coriolis constant, $F_{01}$, which couples the tunnelling states.

The observation that well resolved K-structure suddenly occurs for the K multiplet at ~808.3 $cm^{-1}$ suggests that, in addition to the possibilities considered above, strong localized resonances arc occurring. This extra complication may be due to Coriolis interactions between $\nu_6$ and the combination band at 801.5 $cm^{-1}$ which wc believe can be assigned to v7 + $\nu_{12}$. The combination band appears in the spectra as a C-type band, Accordingly, the upper state of the transition, ie the combination state, must be of A“ symmetry. The shading of the central Q branch at 801.5 is then duc to A’ - A“ > 0. Such a state should exhibit both A and B axis Coriolis interaction with $\nu_6$.

The Coriolis interaction will only affect lines with high values of J and $K_a$. This restriction occurs since the resonances require AJ = O, and the energy oft’set between the band

origins can only be nullified for highly excited rotational states. The central Q branch is sensitive to the coupling between the tunnelling states and to the Coriolis interaction with the combination state. In order to estimate the strength of the interaction wc have scaled the $\xi_A$ and $\xi_B$ values found for $CH_2NH$ (22) by the ratic of the A and B rotational constants in H02N02 and $CH_2NH$. Wc find that inclusion of the Coriolis interaction produces a considerable variation in the "beating" structure seen n the central Q branch, however, with the present parameters wc arc unable to reproduce the degree of irregularity of the experimental spect rum.

Inclusion of Coriolis couplings between ground and excited tunnelling states as well as between the $\nu_6$ and $\nu_7 + \nu_{12}$ states explains only some of the observed complexity of the $\nu_6$ band. Our observation of a substantial temperature dependence in the structure of the strong central Q branch suggests that at least two hot bands arc coincident with $\nu_6$ and arc responsible for much of the spectral complexity. This is consistent with the expectation that a significant population resides in the low-lying vibrational states even at 220 K. The relative populations of these states arc given in Table III for temperatures of 220 K and 296 K. The intense hot band at 802.8 $cm^{-1}$ is believed to involve the lowest lying torsional state and wc assign it as $\nu_6 + \nu_{12} - \nu_{12}$. The identity of the second hot band located at approximately 803.0 $cm^{-1}$ is "more difficult to discern. Among the possible assignments the most likely is v6 $+ \nu_{11} - \nu_{11}$.

In order to show the effects of both of the superimposed hot bands and the nearby fundamental and combination bands wc have simulated the structure of the spectral region near 803 cm-l using the parameters given in Table IV. The resulting spectra at 220 K and 296 K arc shown in figure 7 and figure 2c. From these figures it can bc seen that wc arc now able to provide a good description of the overall observed band behavior. However, wc arc still unable to completely reproduce the degree of irregularity observed in the experimental spectra.

The progress that wc have made to date on the spectral region near 803 $cm^{-1}$ is sufficient to allow for improved attempts at retrieval of atmospheric PNA concentrations from in situ observations of the $\nu_6$ band. In particular, the variation of the atmospherically

prominent Q branch as a function of temperature and pressure can now be reasonably simulated using the present set of line parameters. A line list for the Q branch region is available on request from the authors. Further progress on the analysis of the $\nu_6$ band requires experimental identification of the energies of the two remaining low-lying vibrational levels of PNA.

**Acknowledgements**

The research described in this paper was carried out by the Jet Propulsion Laboratory, California Institute of Technology, under a contract with the National Aeronautics and Space Administration. G. Duxbury was a visiting scientist at the Jet Propulsion Laboratory.

## References


1) D. Weisenstein, M. W. K. Ko, J. M. Rodriquez, and N. D. Sze, Geophys. Res. Lett. 18, 1991-1994 (1991).

2) N.D. Sze and M.K.W. Ko, Atmos. Environ. 15, 1301-1307 (1981).

3) A. Goldman, F.J. Murcray, R. Il. BlatherWick, J.J. Kosters, F.H. Murcray and D.G. Murcray, J. Geophys. Rcs. 94,4945-4955 (1 989).

4) C.P. Rinsland, R. Zander, C.B. Farmer, R.H. Norton, L.R. Brown, J.M. Russell and J.H. Peel, Geophys. Rcs. Lett. 13,761-764 (1 986),

5) R.D. May and R.R. Friedl, submitted to JQSRT.

6) R.D. May and C.R. Webster, J. Mol. Spectrosc. 138, 383-397 (1989).

7) R.A. Kenlcy, P.L. Trevor and B.Y. Yan, J. Am. Chem. Sot. 103, 2203-2206 (1 981 ).

8) F.W. Birss and D.A. Ramsay, Comput. Phys. Commun. 38,83-112 (1984),

9) R.H. Judge, Comput. Phys. Commun. 47,361-363 (1987).

"lo) G. Duxbury, to be published.

11) H.M. Pickett, J. Mol. Spectrosc. 148, 371-377 (1991 ).

12) R.A. Graham, A.M. Winer and J.N. Pitts, Geophys. Res. Lett. 5, 909 (1 978).

13) R.D. May and D.B. Peterson, J. Mol. Spectrosc. 150, 647-649(1991).

14) F. Melen and M. Herman, J. Phys. Chem. Reference Data, 21, 880-881 (1992).

15) A.C. Baldwin and D.M. Golden, J. Phys. Chem. 82,644-647 (1978).

16) R.H. Miller, P.L. Bernitt and I.C. Hisatsunc, Spectrochim. Acts 23A, 223-236 (1967).

17) W, Bell, J, Ballard and G. Duxbury, unpublished work, see (1 7).

18) W. Bell, PhD Thesis, University of Strathclyde, 1991.

19) R. D, May, unpublished results.

20) R.D. Suenram, F.J. Lovas and H.M. Pickett, J. Mol. Spetrosc. 116, 406-421 (1986).

21) H.M. Pickett, J. Chcm.Phys.S6,1715-1726 (1972).

22) L. Halonen and G. Duxbury, J. Chem. Phys. 83, 2078-2090 (1985).

**Figure Captions**

1. The $\nu_7$ band of H02N02 recorded at a temperature of 220K, a pressure of 0.0035 Torr and with a resolution of 1.0 $cm^{-1}$.
2. Overview of the central region of the $\nu_6$ band,
   (a) Experimental spectrum at a temperature 220 K, resolution 0.003 cm-l.
   (b) Simulation with A' = 0.401 $cm^{-1}$, B' = 0.15531 $cm^{-1}$ and C' = 0.15531 $cm^{-1}$ and a band origin of 802.546 cm-l.
   (c) Same as (b) with the addition of the $\nu_7 + \nu_12$ combination band at 801.5 cm-l and two hot bands centered at 802.79 (v6 + $\nu_{12} - \nu_{12}$) and 803.0 cm-l ($\nu_6 + \nu_{11} - \nu_{11}$). The rotational constants used in this simulation are given in Table 4,

   Calculation (b) reproduces the gross features of the experimentally observed spectrum, the P and R branch spacings and the overall degradation of the Q branch. However, it does not reproduce the irregularities in any of the branches. Calculation (c) represents the best fit to the observed spectra given the present state of knowledge regarding the fundamental vibrational frequencies of PNA
3a. Rotational structure of the low J R branches of the $\nu_6$ band in the region 805-806 $cm^{-1}$. The 'oblate' top lines spaced by 2C and the 'prolate' top lines spaced by B+C arc indicated. The near degeneracy of these series at 805.6 $cm^{-1}$ confirms the band origin.
3b. Same as (3a) except for the region 806-807 cm-l.
4. A comparison of observed (a) and calculated (b,c) rotational structure in the R branch region of the $\nu_6$ band. (b), no inversion splitting, calculated using the parameters given in Table II. (c), inversion splitting, equal coupling in the upper and lower states, calculated using sets (a) and (h) of Table IV. Note the increased spreading of the K-structure of the higher J lines in (c), although not as fast as in the experimental spectrum, (a).
5. A comparison of calculated structures in the R branch (a), with the same parameters as for Figure 4c, and (b) with $F_{01}$ increased by a factor of 2 [set (d) in Table IV]. Note the rapid increase in the spacing of the K structure in the second case.
6, The band center of the $\nu_6$ band of H02N02
   (a) Temperature 298 K, resolution 0.006 $cm^{-1}$.
   (b) Simulation of(a) using parameters given in Table IV.
   (c) Temperature 220 K, resolution 0.003 cm-l.
   (d) Simulation of(c) using parameters given in Table IV.

   The main features of the structure arc temperature independent, except for the Q

branch features at ca. 802.8 and 803.0 $cm^{-1}$ which arc markedly reduced in intensity at low temperature.

**Title for Tables**

Table I — A comparison of the vibration frequencies of peroxynitric acid, H02N02, and of fluoronitrate, $FONO_2$, equivalent vibrations arc adjacent horizontally.

Table 11 — Rotational Constants ($cm^{-1}$) for the $\nu_6$ band of H02N02

Table 111 — Relative rotational populations of selected vibrational states of PNA at 296 K and 220 K,

Table IV — Rotational Constants ($cm^{-1}$) used for the calculations of the simulated structure of the v6 band of H02N02 when different possible interactions are included. The two inversion components are given for each constant.

**Table I**

A comparison of the vibration frequencies of peroxynitric acid, $HO_2NO_2$, and of fluoronitrate, $FONO_2$, equivalent vibrations are adjacent horizontally.

| Near sym. | Approximate type of mode | Vib. | $\nu$ $(HO_2NO_2)/cm^{-1}$ | | $\nu(FONO_2)/cm^{-1}$ b |
|---|---|---|---|---|---|
| $C_s$ | | | | | |
| a' | OH stretch | v] | 3540.1[a] | | |
| | N02 asym. stretch | $\nu_2$ | 1728.3[a] | $\nu_1$ | 1759.1 |
| | OH bend | *V3* | 1396.9a | | |
| | N02 sym. stretch | *V4* | 1304.2a | $\nu_2$ | 1300.9 |
| | O-O stretch | *V5* | 940[c] | *V3* | 927.7 |
| | N02 scissors | $\nu_6$ | 802.543[d] | *V4* | 803.7 |
| | NO stretch | $\nu_7$ | 648[d] | *V5* | 633.0 |
| | N02 rock | $\nu_8$ | 458[d] | $\nu_6$ | 454.5 |
| | NOO dcf. | *V9* | | *V7* | 302.6 |
| a" | N02 wag | $\nu_{10}$ | 722[c,d] | $\nu_8$ | 708.5 |
| | OH torsion | $\nu_{11}$ | | | |
| | NOO torsion | $\nu_{12}$ | 153.5[d,c] | V9 | 151.6 |

a R.A. Graham, A.M. Wirier and J.N. Pitts, Geophys. Rcs. Lett. 5, 909 (1978).

b R.H. Miller, P.L. Bernitt and I.C. Hisatsunc, Spectrochim. Acts 23a, 223-236 (1967).

c R.D. May and D.B. Peterson, J. Mol. Spcctrosc. 150, 647-649 (1991).

d This work.

c R.D. Suenram, F.J. Lovas and H.M. Pickett, J. Mol. Spectrosc. 116, 406-421 (1986).

**Table 11**

Rotational Constants ($cm^{-1}$) for the $\nu_6$ band of $HO_2NO_2$

| Parameter | Ground State[a] | $\nu_6$ |
|---|---|---|
| $\nu_0$ | ------- | 802.543 (5) |
| A | 0.400093 | 0.40101 (7) |
| B | 0.155611 | 0.15549 (13) |
| c | 0.113170 | 0.11300 (2) |

a) Ground state constants derived from microwave results (18) averaging over the inversion components.

b) Quoted errors arc three standard deviations. Determined constants were obtained directly from the least squares analysis of the low J and Ka transitions,

**Table 111**

Relative rotational populations of selected vibrational states of PNA at 296 K and 220 K.

| Mode | Frequency ($cm^{-1}$) | Relative Population (298 K) | Relative Population (220 K) |
|---|---|---|---|
| $\nu_{12}$ | 153.5 | 0.478 | 0.367 |
| $\nu_{11}$ | -200 | 0.382 | 0.271 |
| V9 | -300 | 0.236 | 0.141 |
| $2\nu_{12}$ | -307 | 0.22$ | 0.134 |
| $\nu_{11} + \nu_{12}$ | 353 | 0.183 | 0.099 |
| $2\nu_{11}$ | -400 | 0.146 | 0.074 |
| $\nu_8$ | 458 | 0.110 | 0.050 |
| $3\nu_{12}$ | 460.5 | 0.109 | 0.049 |

**Table IV**

Rotational Constants (cm-l ) used for the calculations of the simulated structure of the $\nu_6$ band of H02N02 when different possible interactions are included. The two inversion components arc given for each constant.

| Parameter | Ground State (a) | $\nu_6$ (b) | $\nu_7 + \nu_{12}$ (c) | $\nu_6 + \nu_{12} - \nu_{12}$ | $\nu_6 + \nu_{11} - \nu_{11}$ |
|---|---|---|---|---|---|
| $\nu_0$ | ------ | 802,543 | 801,548 | 802.794 | 803.004 |
| | 0.0594623 | 802,602 | 801.608 | | 803.063 |
| A | 0<4000934 | 0.401003 | 0.40030 | 0.39814 | 0.400009 |
| | 0.4000868 | 0.400993 | 0.40028 | 0,39835 | 0.400087 |
| B | 0.1556158 | 0.155410 | 0.155615 | 0.15555 | 0.155616 |
| | 0,1556079 | 0.155410 | 0.155607 | 0.15555 | 0.155608 |
| c | 0.113318 | 0.112990 | 0.113318 | 0.113476 | 0.113318 |
| | 0.113317 | 0.112990 | 0.113316 | 0.113376 | 0.113317 |
| $F_{01} \times 10^4$ | 7.02419 | 7.02419 | 7.02419 | | |
| | | 14.048 (d) | | | |
| $\xi_a$ | -- | 0.01 (c) | 0.01 (c) | | |
| $\xi_b$ | -- | 0.005 (c) | 0.005 (c) | | |

a) From reference (18)

b) Constants from least squares fit adjusted using ground state splitting of rotation constants. $F_{01}$ from ground state.

c) Band origin estimated from observed spectra.

d) Inversion coupling constant twice that in the ground state.

e) Coriolis constants estimated by scaling from CH2NH, reference (20).

f) All centrifugal distortion constants frozen at ground state values.

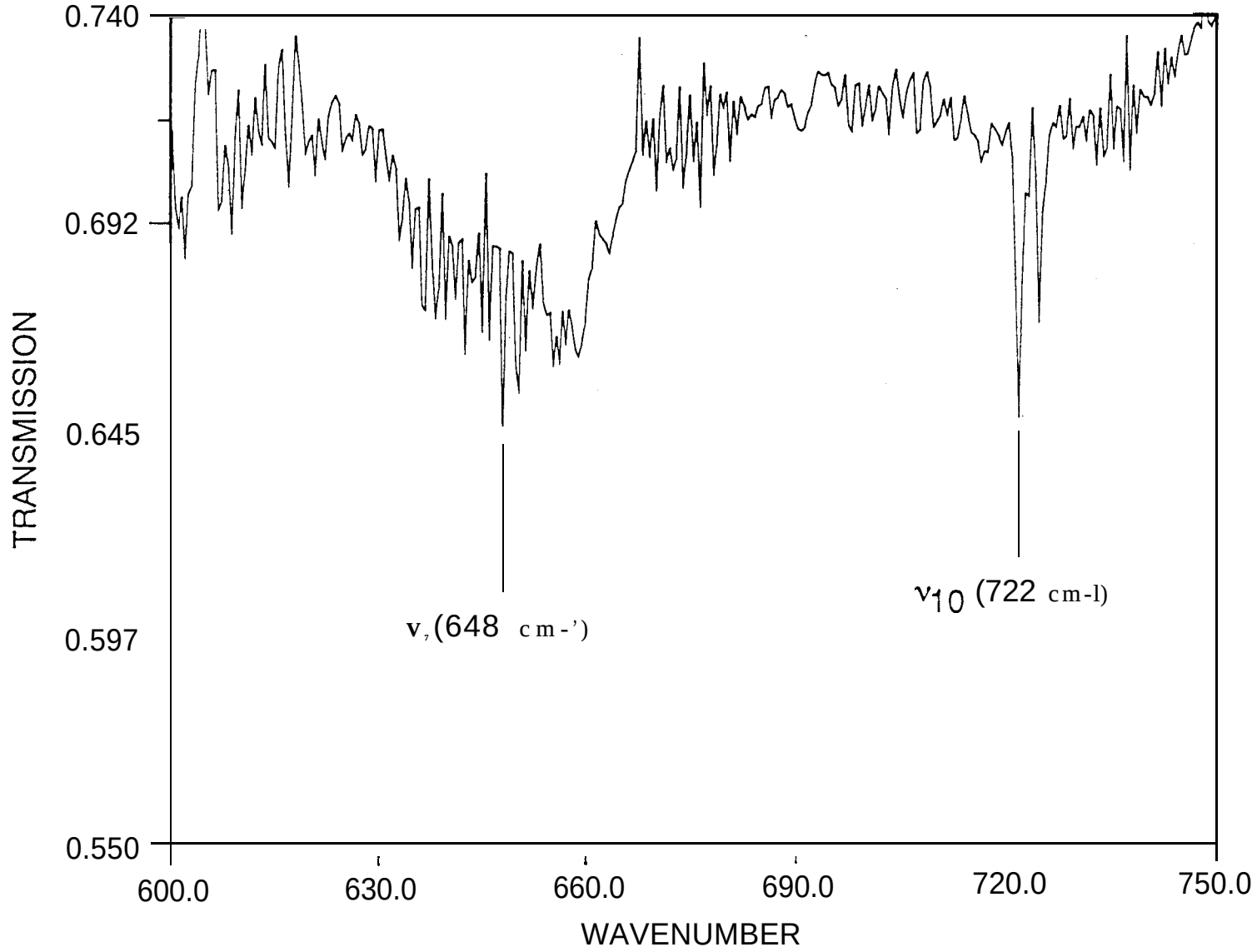
0.740
0.692
0.645
0.597
0.550
TRANSMISSION
600.0
630.0
660.0
690.0
720.0
750.0
WAVENUMBER
v, (648 cm-')
v10 (722 cm-l)

Figure

Figure 2a

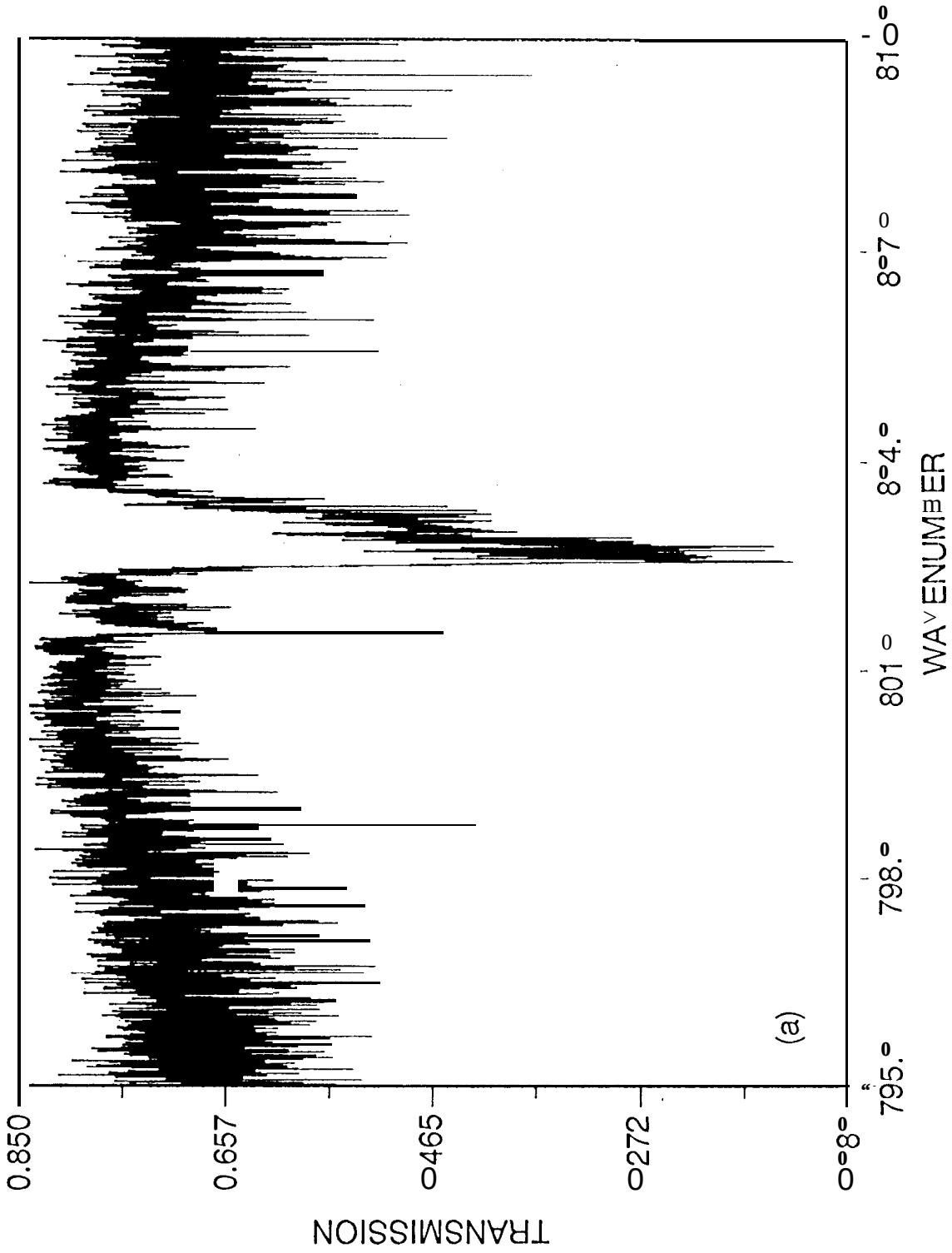
TRANSMISSION
0.850
0.657
0.465
0.272
0.080
795.0
798.0
801.0
804.0
807.0
810.0
WAVENUMBER
(a)

Figurc2b

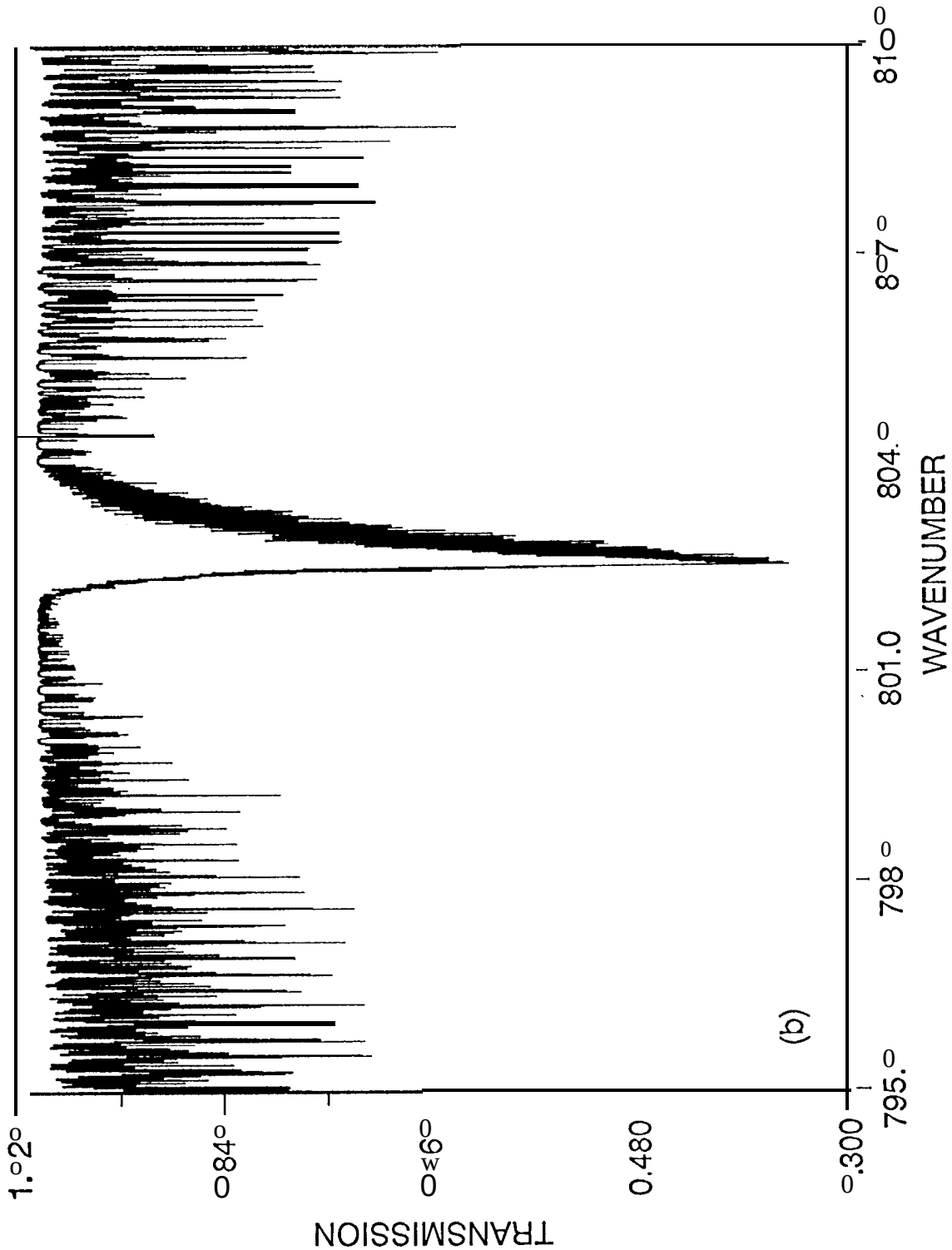
TRANSMISSION
1.0
0.840
0.960
0.480
0.300
795.0
798.0
801.0
804.0
807.0
810.0
WAVENUMBER
(b)

Figure 2c

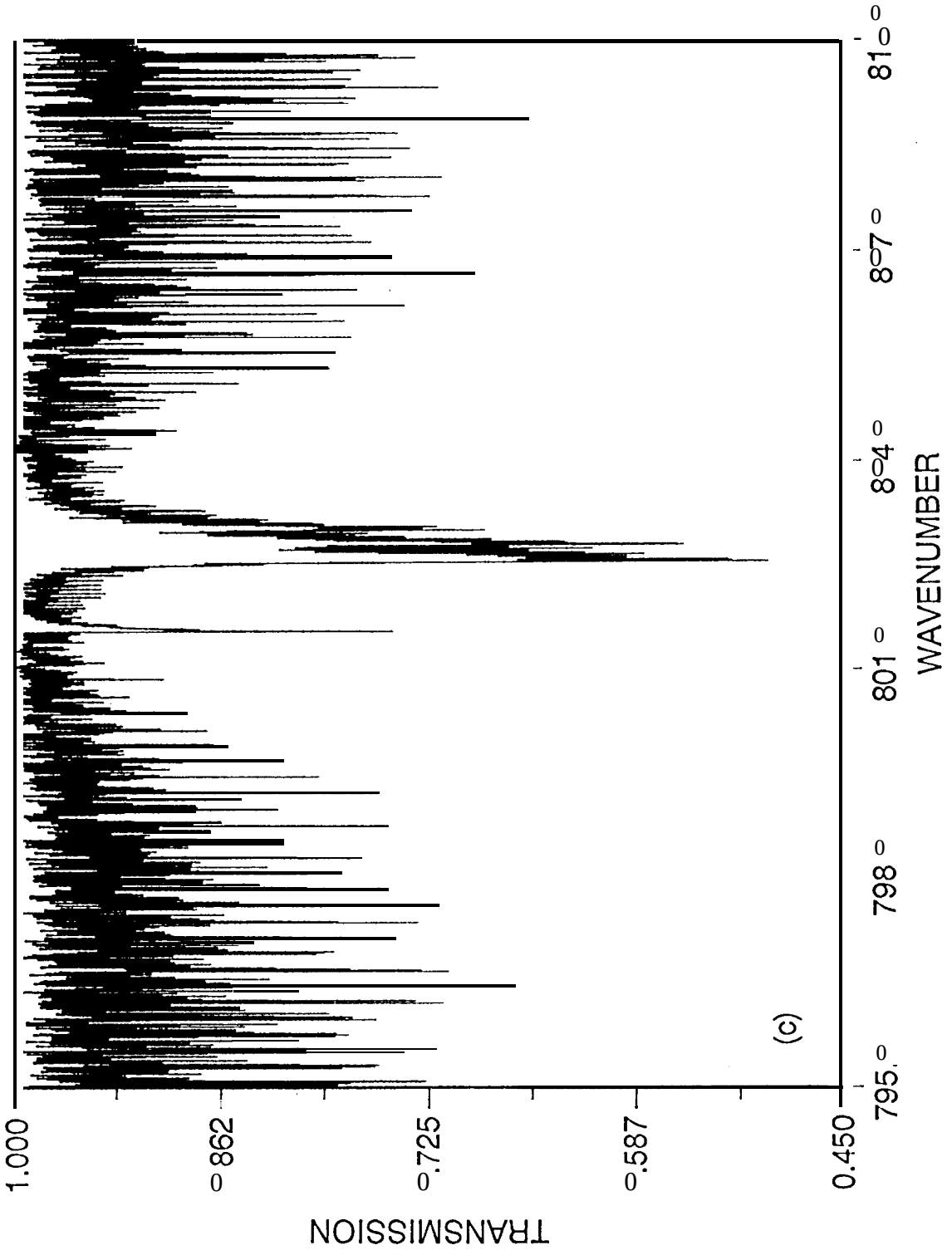
TRANSMISSION
1.000
0.862
0.725
0.587
0.450
WAVENUMBER
795.0
798.0
801.0
804.0
807.0
810.0
(c)

Figure 3a

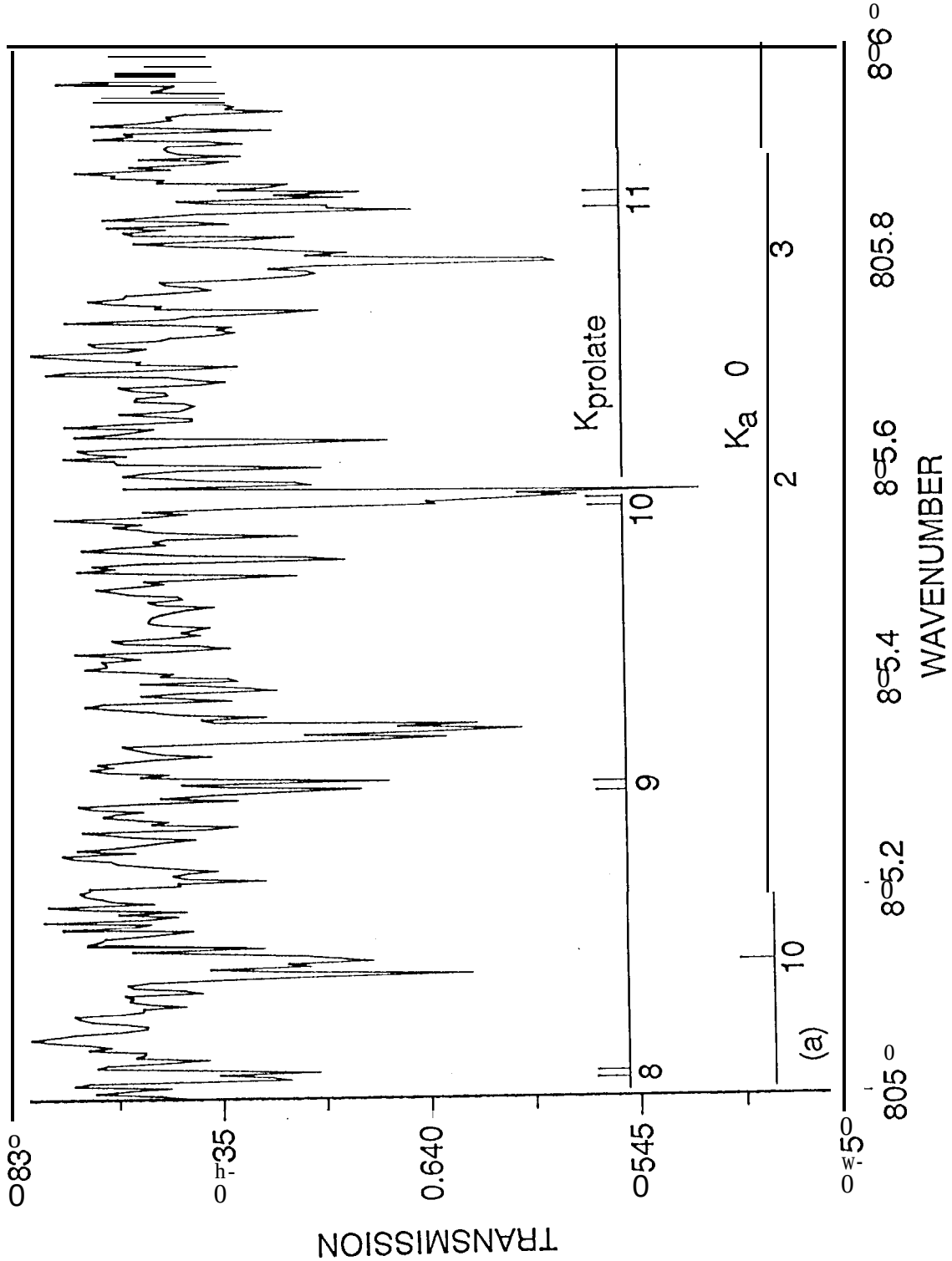
TRANSMISSION
WAVENUMBER
805.2
805.4
805.6
805.8
(a)
$K_a$ 0
$K_{prolate}$
8
9
10
11
2
3
10

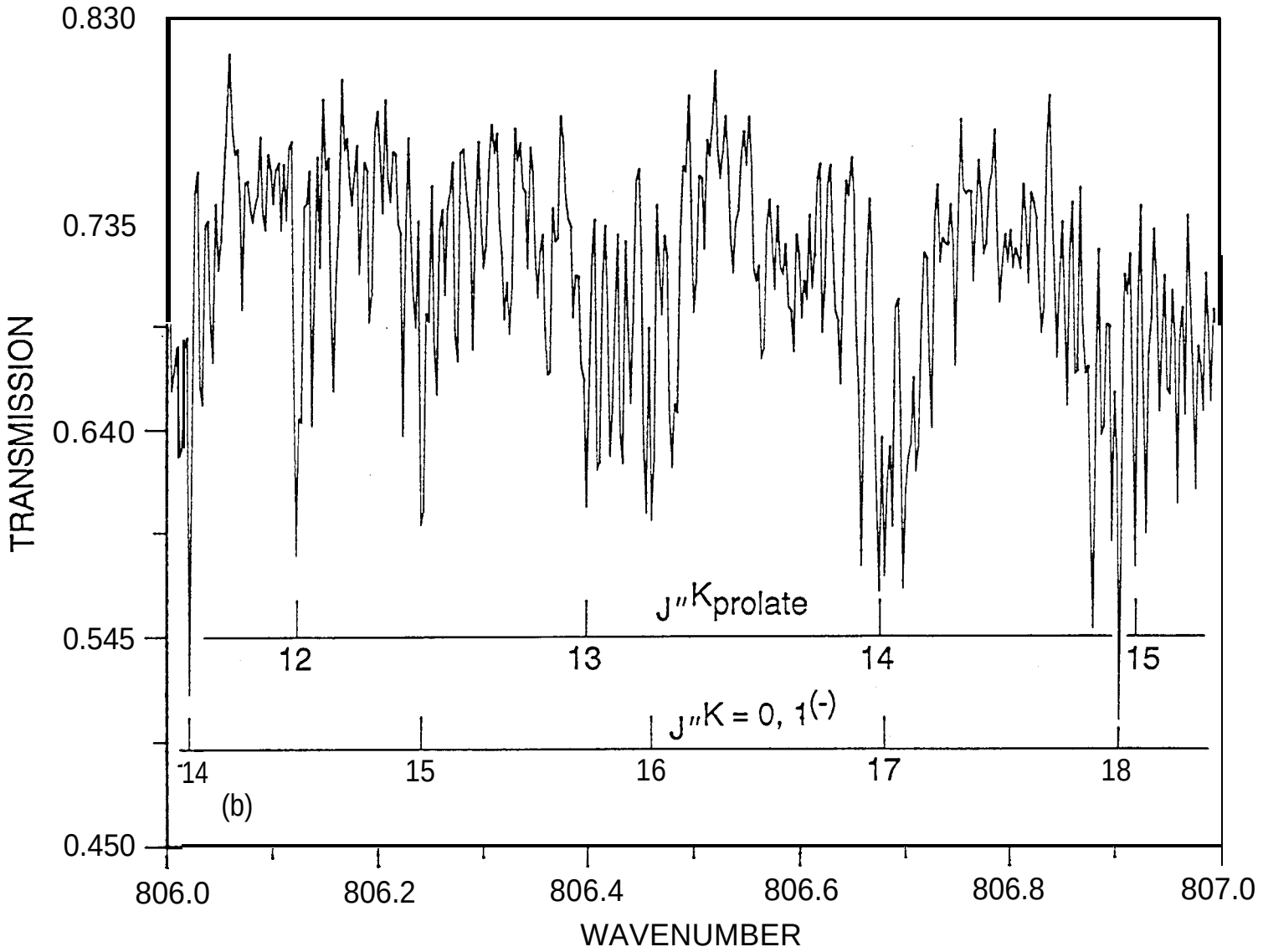
0.830
0.735
0.640
0.545
0.450
TRANSMISSION
J″Kprolate
12
13
14
15
J″K = 0, 1(-)
14
15
16
17
18
(b)
806.0
806.2
806.4
806.6
806.8
807.0
WAVENUMBER

Figure 3b

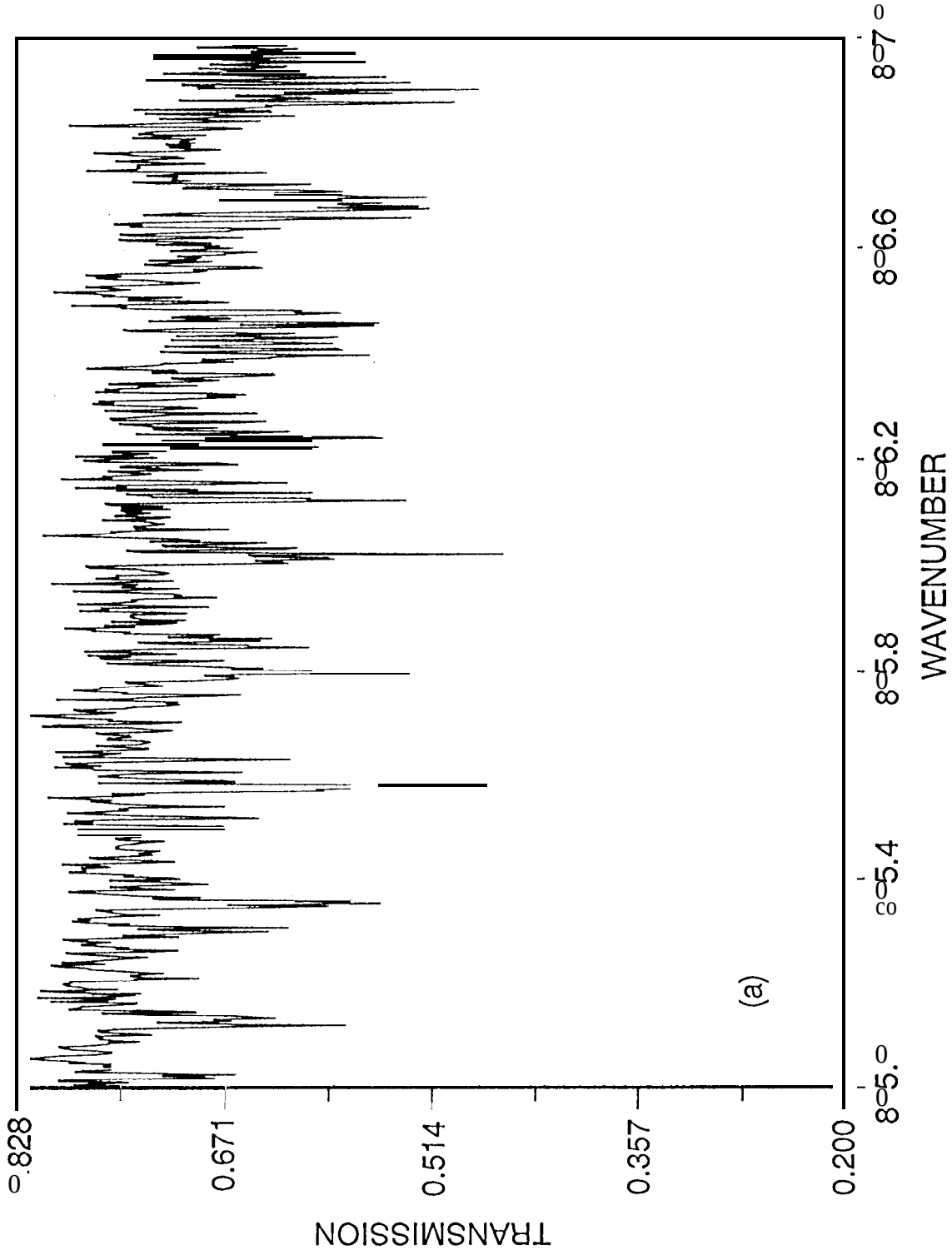
TRANSMISSION
0.828
0.671
0.514
0.357
0.200
WAVENUMBER
805.0
805.4
805.8
806.2
806.6
807.0
(a)

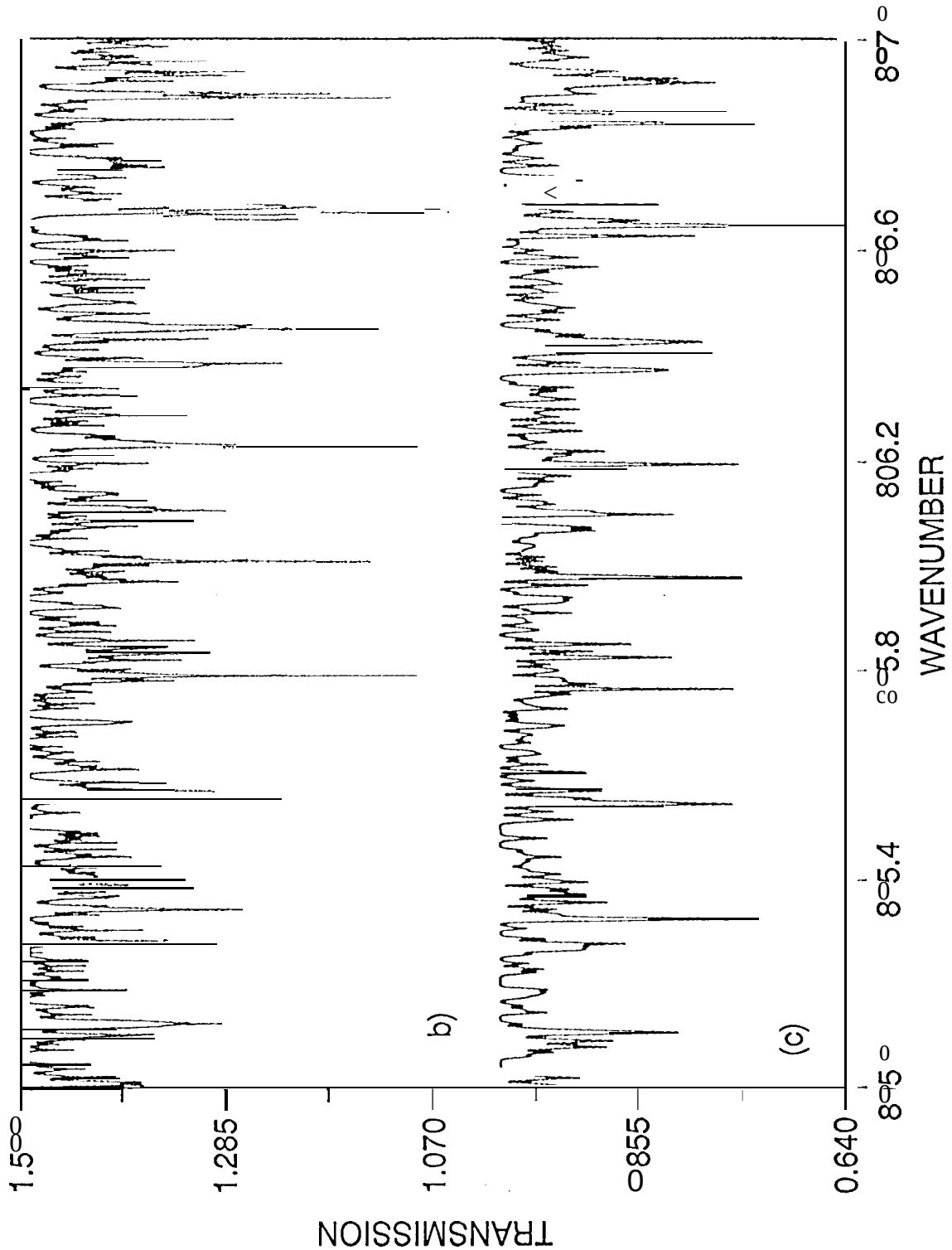
TRANSMISSION
1.500
1.285
1.070
0855
0.640
b)
(c)
805.0
805.4
805.8
806.2
806.6
807.0
WAVENUMBER

Figure 5a and 5b

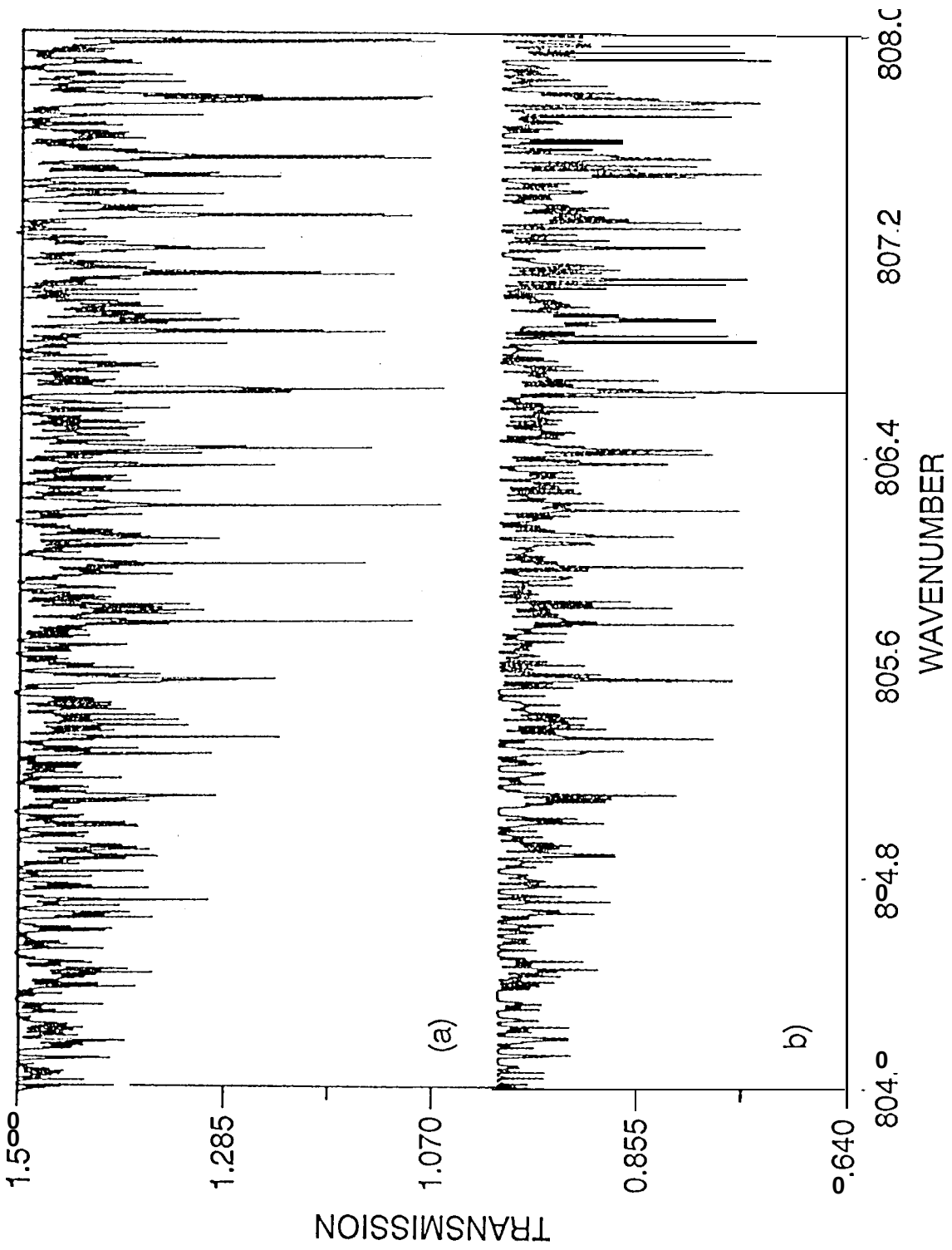

**Figure 6a**

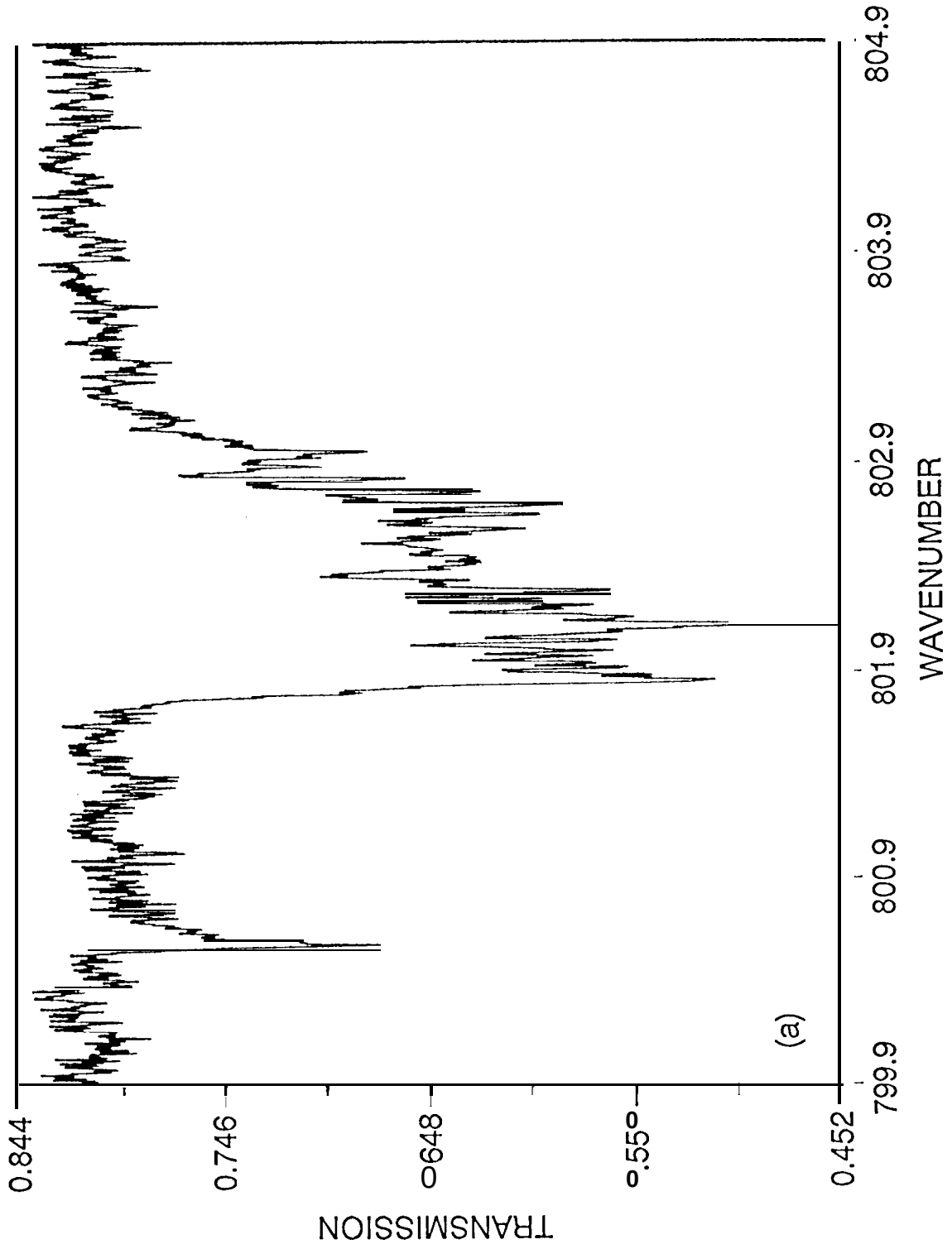
TRANSMISSION
0.844
0.746
0648
0.55o
0.452
799.9
800.9
801.9
802.9
803.9
804.9
WAVENUMBER
(a)

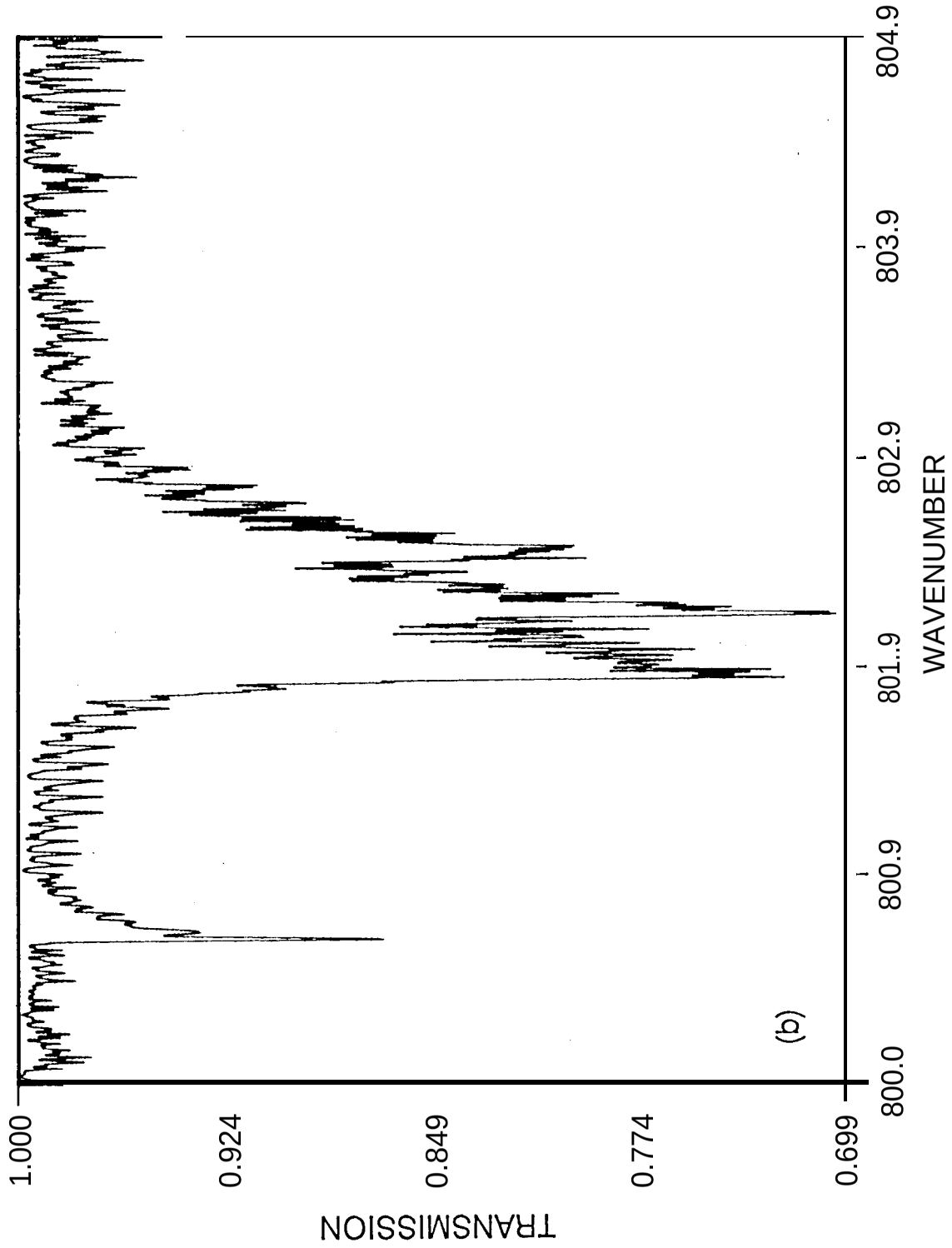
1.000
0.924
0.849
0.774
0.699
TRANSMISSION
800.0
800.9
801.9
802.9
803.9
804.9
WAVENUMBER
(b)

Figure 6c

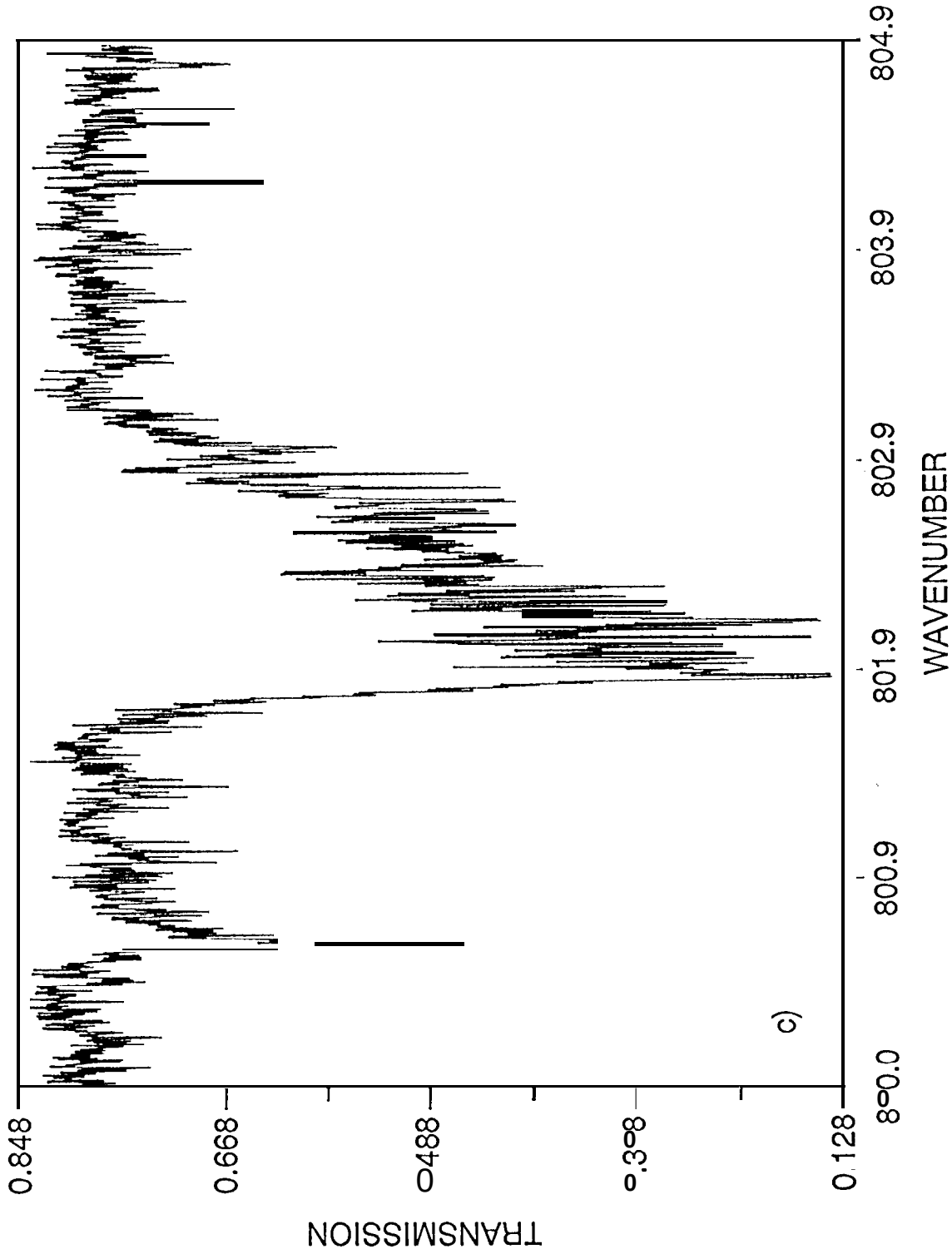
TRANSMISSION
0.848
0.668
0488
0.3°8
0.128
8°0.0
800.9
801.9
802.9
803.9
804.9
WAVENUMBER
c)

Figure 6d

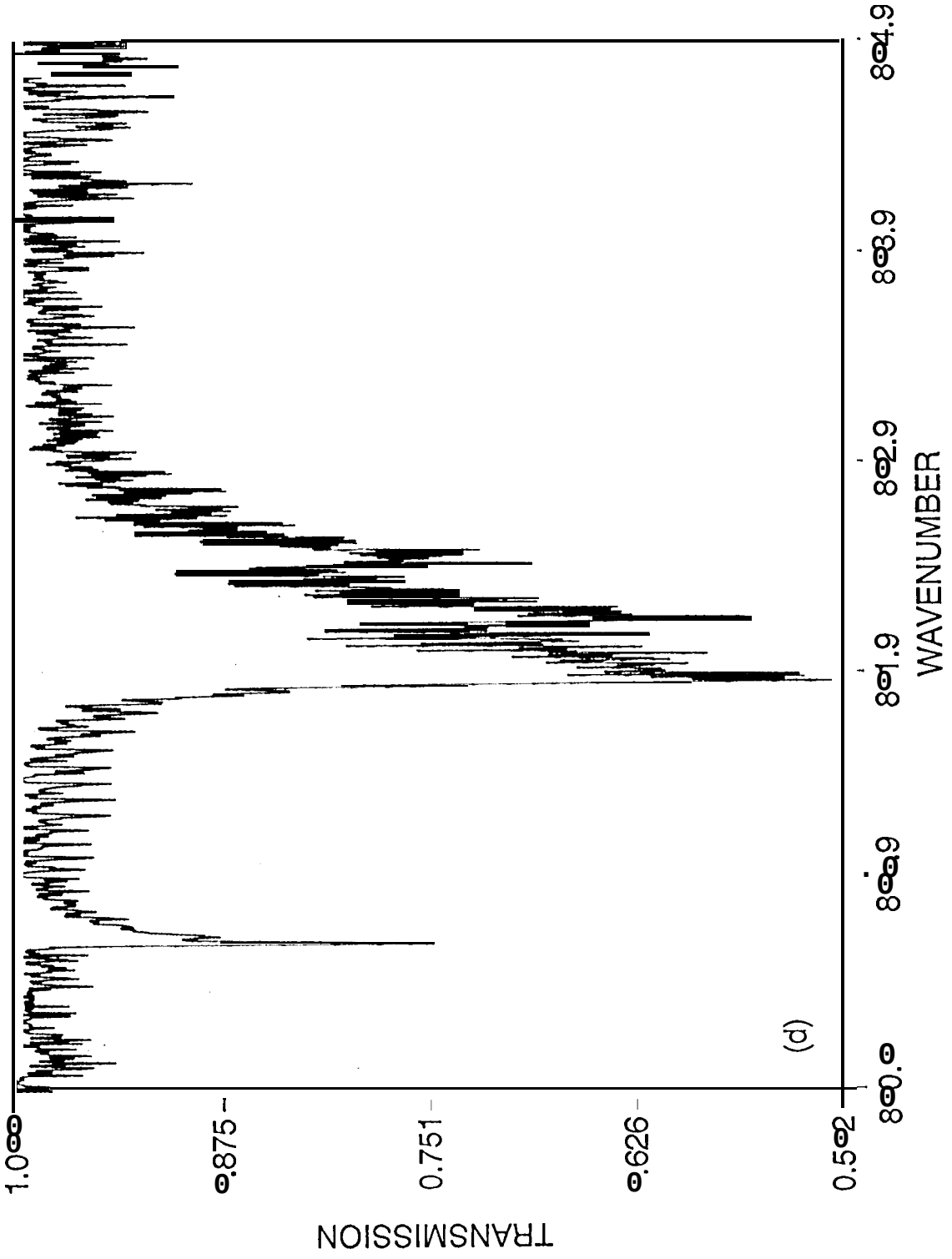
TRANSMISSION
1.000
0.875
0.751
0.626
0.502
800.0
801.9
802.9
803.9
804.9
WAVENUMBER
(d)